THE LAGRANGIAN POINTS OF THE REAL EARTH-MOON SYSTEM *

ENRIC CASTELLÀ AND ÀNGEL JORBA

Departament de Matemàtica Aplicada i Anàlisi, Universitat de Barcelona, Gran Via 585, 08007 Barcelona, Spain. E-mail: angel@maia.ub.es

In this note we discuss the motion of a particle near the Lagrangian points of the real Earth-Moon system. We use, as real system, the one provided by the JPL ephemeris: the ephemeris give the positions of the main bodies of the solar system (Earth, Moon, Sun and planets) so it is not difficult to write the vectorfield for the motion of a small particle under the attraction of those bodies. Numerical integrations show that trajectories with initial conditions in a vicinity of the equilateral points escape after a short time. On the other hand, the Restricted Three Body Problem is not a good model for this problem, since it predicts a quite large region of practical stability. Therefore, we introduce an analytic model that can be written as a quasi-periodic perturbation of the Restricted Three-Body Problem, that tries to account for the effect on the Sun and the eccentricity of the Moon. Then, we compute some families of normally elliptic 3-D invariant tori at some distance from the triangular points, that give rise to regions of effective stability. By means of numerical simulations, we show that these regions seem to persist in the real system, at least for time spans of 1000 years.

1. Introduction

One of the simplest models for this problem is the well known Restricted Three Body Problem (from now on, RTBP). The RTBP models the motion of a particle under the gravitational attraction of the Earth and Moon (the primaries), under the following assumptions: i) the particle is so small that it does not affect the motion of Earth and Moon; and ii) Earth and Moon are point masses that revolve in circular orbits around their common centre of mass. It is well known[14] that, in a rotating frame, the RTBP has five equilibrium points: three of them lay on the x axis (they are called collinear points, Eulerian points, or $L_{1,2,3}$), and the other two form an equilateral

*Work supported by the MCyT grant BFM2000–0623, the CIRIT grant 2001SGR–70 and DURSI.

triangle (in the (x, y) plane) with Earth and Moon (they are called triangular points, Lagrangian points or $L_{4,5}$). If the ratio of the masses of the primaries is small enough (this includes the Earth-Moon case), the triangular points are linearly stable. Under very general conditions,[7,13,3,1] there exists a neighbourhood of these points such that any initial condition inside this neighbourhood produces a trajectory that remains close to the point for huge intervals of time. This behaviour (stability for finite but very large time intervals) is known as "effective stability".

On the other hand, we can consider one of the most accurate models of the Solar system now available, which is the JPL Ephemeris. Even if this model cannot be studied analytically, it can be integrated numerically. The main question is what features of the RTBP transfer to the JPL model. Clearly the Lagrangian points are not equilibrium points anymore when we take into account the real motion of Earth and Moon, and the presence of Sun and planets. Moreover, direct numerical integration of JPL model shows that the neighbourhood of the triangular points is no longer stable for the JPL model, since nearby trajectories escape after a short time[6]. Therefore, the RTBP is not a good model to study this problem because it displays a quite different qualitative behaviour.

For this reason, we will introduce some improved models. The first one is the so called Bicircular Problem (from now on, BCP). This model can be seen as a time dependent periodic perturbation of the RTBP, includeing the direct effect coming from the Sun.[5] Our first goal will be to use the BCP to describe some properties of the real model. In particular, we will compute, for the BCP, families of quasi-periodic solutions near the equilateral points. We will see that some of them are unstable, while some others are stable. Those stable solutions are found at some distance from the equilateral points. It is known[11,10] that, under generic hypotheses, stable quasi-periodic solutions are surrounded by regions of effective stability. The size and shape of these regions will be estimated by means of numerical simulations. Finally, we will show, by means of numerical simulations, that some of these stability regions found in the BCP model seem to subsist in the JPL model, at least for time spans of 1000 years.

To improve the previous results, we will also introduce the Circular Elliptic Problem (CEP), that can be written as a quasi-periodic time dependent perturbation of the RTBP, and includes the main effect from the Sun and the eccentricity of the Moon. We will show how this model allows to compute slightly larger stability regions.

2. The Bicircular Problem

Let us assume that Earth and Moon are point masses that revolve in circular orbits around their common centre of mass (as in the RTBP), and let us also assume that this centre of mass revolves in a circular orbit around the Sun (also considered as a point mass) fixed at the origin. We are also assuming that the motion of the three bodies is coplanar. The purpose of the Bicircular Problem is the study of the motion of an infinitesimal particle under the attraction of these three main bodies. It is usual to take the same reference frame as in the RTBP. So, in this system of reference, Earth and Moon are fixed on the x axis while the Sun is turning around the Earth-Moon centre of masses, that is located at the origin. Therefore, we can look at the BCP as a periodic time dependent perturbation of the RTBP. In fact, we will write a parameter ε in front of the mass of the Sun so that, moving this parameter, our model goes from the RTBP ($\varepsilon = 0$) to the BCP ($\varepsilon = 1$).

Now, let us focus on the L_5 point (due to the symmetries of the RTBP and BCP, the same results will hold for L_4; of course, this does not apply to the real system). As the vector field of the BCP does not vanish on L_5, this point is not longer an equilibrium solution. It is not difficult to prove that, under a generic non-resonance condition (satisfied in this case) and assuming ε small enough, L_5 is replaced by a periodic orbit with the same period as the perturbation. This orbit tends to L_5 when ε tends to zero.

Let us consider now the Poincaré section defined by $t = 0 (\mathrm{mod}\, T_S)$, where T_S is the period of the time-dependence (i.e., the Sun) in the BCP and let us call P_ε the corresponding Poincaré map. Now, let us compute the fixed points of P_ε for ε ranging between 0 and 1. The results are displayed in Figure 1 (left), where the horizontal axis shows the x coordinate of the fixed point and the vertical axis refers to the value of ε. Note that, for $\varepsilon = 1$ (the BCP), there are three fixed points of P_ε that are close to L_5. The (x, y) projection of the corresponding periodic orbits for the flow are displayed in Figure 1 (right). It is easy to see that orbit PO1 is unstable, while orbits PO2 and PO3 are linearly stable. Moreover, the three periodic orbits have an elliptical mode contained in the $(z, \dot{z})$ plane (this corresponds to librations perpendicular to the plane of motion of the Moon around the Earth). In what follows, we will refer to this mode as the vertical mode of the corresponding periodic orbit. For more details about the BCP we refer to Simó et al.[12,4]

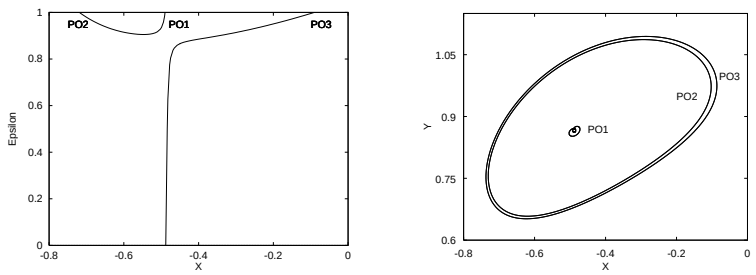

Figure 1. Left: Continuation of the periodic orbit that replaces L_5 in the BCP. Right: The three periodic orbits that appear on the left plot for $\varepsilon = 1$.

2.1. *Families of quasi-periodic motions*

As mentioned before, L_5 is a linearly stable equilibrium point of the RTBP. Moreover, the linearization of the vector field at this point can be described as the product of three linear oscillators: two of them are contained in the (x, y) plane, and the third one moves exactly on the z axis. In what follows, let us focus on this vertical oscillation of the RTBP that is contained in the z axis. The well-known Lyapunov centre theorem implies that this vertical oscillation of the linearized system can be extended into the complete RTBP, giving rise to a family (the Lyapunov family) of periodic orbits, that we will refer to as the vertical family.

Let us look at the BCP as a (periodic) perturbation of the RTBP. If the perturbing parameter ε is small enough, we have already mentioned that L_5 becomes a small periodic orbit (with the frequency of the Sun in the BCP). Moreover, it is known[11] that the vertical family of periodic orbits becomes a (Cantor-like) family of quasi-periodic orbits, that will be called the vertical family of quasi-periodic solutions. These solutions have two basic frequencies: the first coming from one of the periodic orbits of the vertical family and the second being the frequency of the Sun. For definiteness, we will call VF1, VF2 and VF3 to the vertical families born in PO1, PO2 and PO3 respectively.

These three families can be accurately computed by means of numerical methods.[4,9] Note that the families VF1 and VF2 are connected, as it is suggested by the diagram in Figure 1 (left). The gaps that conform the Cantor structure of these curves are too small to be seen at this scale.

As PO1 is unstable, we expect that the tori in VF1 are also unstable, at least for moderate values of the vertical amplitude. PO2 and PO3 are stable orbits so, under generic conditions, it is expected that most of the

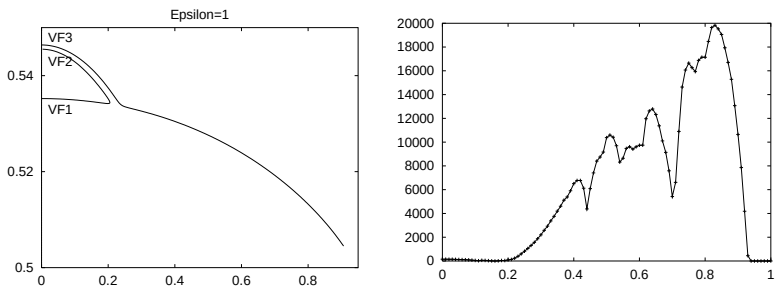

Figure 2. Left: vertical families of invariant tori for the BCP. The plot shows the value of the coordinate $\dot{z}$ of the invariant curve when $t = 0$ and $z = 0$, vs. the rotation number. Right: Size of the stability region for the VF3 family. the plot shows the value of the $\dot{z}$ coordinate vs. the number of initial conditions inside the region.

tori in families VF2 and VF3 with a small vertical amplitude are also stable

2.2. *Stability regions*

As it has been mentioned before, a stable quasi-periodic trajectory is surrounded by a region of effective stability. Here we will try to estimate this region by means of a numerical simulation. To select a mesh of initial conditions around a given solution, let us consider the map P_ε defined before. Note that a (vertical) quasi-periodic solution corresponds to an invariant circle of P_ε that crosses transversally the plane $z = 0$ in two points, with different signs for $\dot{z}$. So, let us select the (unique) point on the invariant curve having $z_0 = 0$ and $\dot{z}_0 > 0$ (this value of $\dot{z}_0$ is, in fact, the value displayed on the vertical axis of Figure 2). In this way, we select a unique point on each quasi-periodic solution.

The mesh used is of the kind $(x_{ij}, y_{ij}, 0, \dot{x}_0, \dot{y}_0, \dot{z}_0)$, where the values $(\dot{x}_0, \dot{y}_0, \dot{z}_0)$ correspond to a given quasi-periodic solution (see above), and x_{ij} and y_{ij} are distributed around the corresponding values (x_0, y_0). In fact, these values are taken as $x_{ij} = r_i \cos\alpha_j + \mu$, $y_{ij} = r_i \sin\alpha_j$, where r_i and α_j are equally spaced. Then, we numerically integrate the trajectories of the BCP starting on each point of the mesh. If the trajectory does not cross the $y = -0.5$ plane, and does not approach collision neither with Earth nor Moon during the integration time, we take the initial condition as belonging to the stability region. Note that, in this way, we produce a 2-D slice instead of the full region.

We have done an extensive numerical simulation for the trajectories in the families VF2 and VF3 (they mostly contain linearly stable tori), during

a time interval of 15000 revolutions of the Moon around the Earth. The results show the existence of large stability regions.[8] Here we will only focus on the family VF3, since the corresponding regions are bigger. These results are summarized in Figure 3. As the mesh has the same size in all the cases, the number of initial conditions corresponding to non-escaping trajectories is a good estimate for the size of the region. Note that the region is neglectable when $\dot{z} < 0.23$ or $\dot{z} > 0.93$. The boundary of these regions is quite sharp, and they are almost not affected by an increasing of the integration time. This phenomenon is known to happen in similar situations.[12] To show the shape of these regions, Figure 3 shows (slices for) a couple of regions, $\dot{z} = 0.58$ and $\dot{z} = 0.83$. Both plots display the (x, y) coordinates of the points in these regions. The explored region has been marked with a semi-circular box.

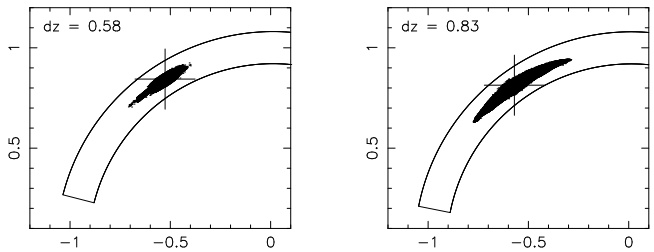

Figure 3. Computed stability regions for the BCP, for the cases $\dot{z} = 0.58$ and $\dot{z} = 0.83$. The initial quasi-periodic solution is marked with a big "+" sign.

3. The stability regions of the BCP in the JPL model

A natural question is whether these regions persist in the real system. To this end, we have repeated the above simulations around the family VF3 using the JPL ephemeris (file DE406), for a time interval of 1000 years. Here, the initial integration time is the first full Moon of year 2000 (this is to have a relative position of Earth, Moon and Sun similar to the one of the BCP when $t_{BCP} = 0$).

The results are summarized in Figure 4. Note that the JPL model does not have the above-mentioned symmetries between the triangular points so we have different plots for them. The horizontal axis refers to the $\dot{z}$ coordinate of the torus in the Poincaré section P_ε of the BCP, as it has been previously introduced. The vertical axis contains the number of points

of the initial mesh that do not escape after several time intervals, ranging from 500 to 1000 years. As all the meshes used have the same density, the number of surviving points can be considered an estimate on the size of the stable region. In this case, the boundaries of the stability region are not as sharp as in the BCP case (there is a small but noticeable leaking of stable initial conditions when the integration time increases).

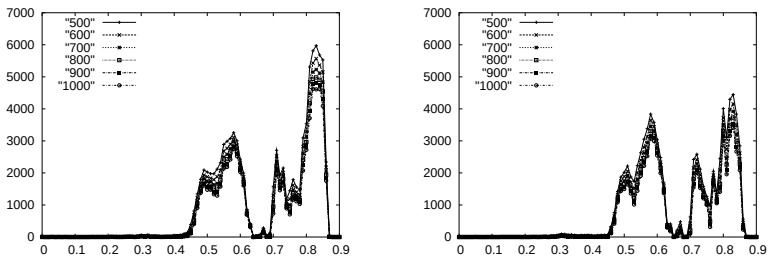

Figure 4. Size of the stability region in the JPL model, for L_4 (left) and L_5 (right). We display the value of the $\dot{z}$ coordinate vs. number of non-escaping initial conditions.

Note that, according to Figure 4, the stability region has a relevant size for the values $\dot{z} = 0.58$ and $\dot{z} = 0.83$. In these simulations, we have used the same mesh as in the BCP problem, so it is possible to compare the sizes of these regions. Although there is a strong reduction in size (w.r.t. the BCP), the number of remaining points is still significative. Figure 5 shows the results of the simulations for the cases $\dot{z} = 0.58$ and $\dot{z} = 0.83$. As before, the horizontal (x) and vertical (y) axis are RTBP coordinates (that is, the unit of distance is the Earth-Moon distance).

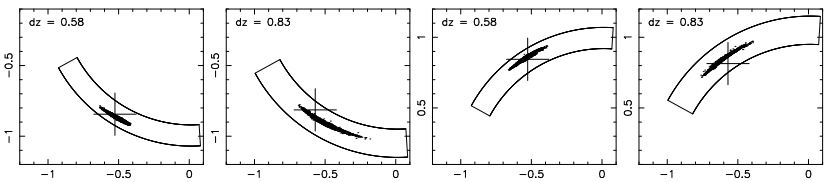

Figure 5. Stability region for the JPL model, for L_4 and $\dot{z} = 0.58$ (1st plot), for L_4 and $\dot{z} = 0.83$ (2nd plot), for L_5 and $\dot{z} = 0.58$ (3rd plot) and for L_5 and $\dot{z} = 0.83$ (4th plot). The box corresponds to the explored region. The initial condition corresponding to the quasi-periodic solution is marked with a big "+" sign.

4. The Circular-Elliptic model

This model is similar to the Bicircular Problem, but now Earth and Moon revolve in elliptic orbits around their centre of masses, that moves in a circular orbit around the Sun. Then, using similar coordinates and units, the motion of the particle is described by a Hamiltonian system that depends on time, in a quasi-periodic way. This quasi-periodic dependence has two basic frequencies, namely the synodical period of the Sun (as in the BCP) and the eccentricity e of the Moon. In particular, if we set $e = 0$, we recover the BCP model.

We proceed as for the BCP model. This is, we first compute the (now quasi-periodic) solutions that replace the triangular point (see Fig. 6). The computation of the reduced Floquet matrix of these solutions[9] shows that T2 and T3 (see Fig. 6) are linearly stable, while T1 is unstable. Now, the vertical family consists of 3-D invariant tori. Due to the high number of Fourier terms to be considered, we have parallelized the method used for the BCP (the details will appear elsewhere).

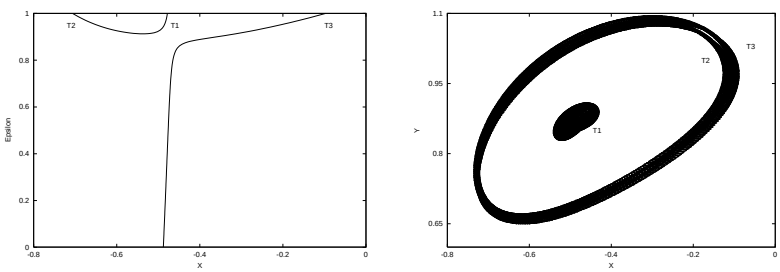

Figure 6. Left: Continuation of the tori that replaces L_5 in the CEP. Right: The three tori of the left plot for $\varepsilon = 1$.

The vertical families are displayed in Fig. 7. Note that now, some of the gaps in the families are visible. In particular, in Fig. 7, right, we can see some gaps due to 1:1 internal–normal resonances.[2] As before, we have done extensive numerical simulations to compute the region of effective stability around these familes. The results are used in the next section as initial conditions for a new simulation in the JPL model.

5. The stability regions of the CEP in the JPL model

We have done the same simulations as in Section 3, but using the initial conditions obtained from the CEP model. The results are summarized in

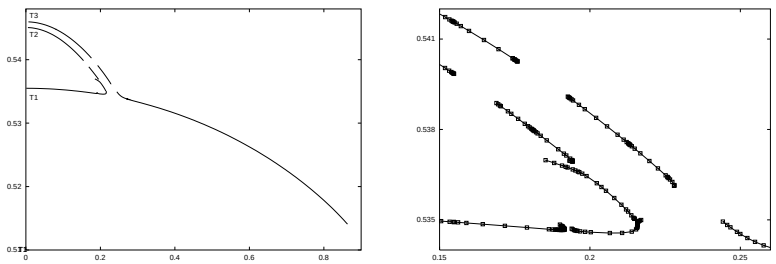

Figure 7. Left: The vertical families of 3-D tori. Right: Magnification of the left plot, the boxes denote the computed tori. The horizontal axis is the $\dot{z}$ coordinate, and the vertical axis displays one of the frequencies.

Fig. 8. Note that the size of these regions is slightly larger than the one obtained from the BCP data. This is because the CEP model is closer to reality (i.e., JPL ephemeris) than BCP and, hence, its prediction about the location of the stability region is more accurate.

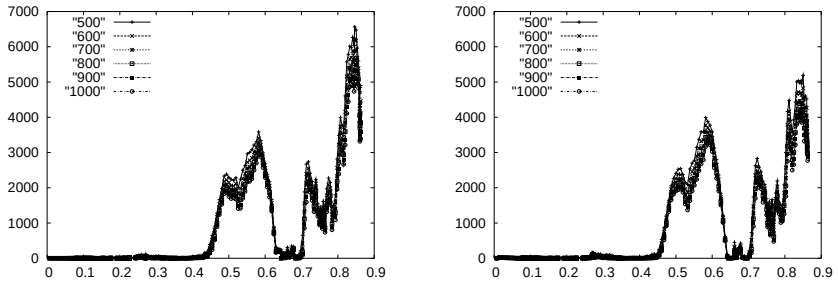

Figure 8. Size of the stability region in the JPL model, for L_4 (left) and L_5 (right). Horizontal axis: value of the $\dot{z}$ coordinate. Vertical axis: number of non-escaping initial conditions. Compare with Fig. 4.

6. Conclusions

The main purpose of this work has been to show the existence of regions of practical stability near the equilateral points of the real Earth-Moon system. The methodology is based on obtaining a first guess for these regions by applying very recent results and techniques from Hamiltonian dynamical systems to suitable intermediate models. These regions are tested numerically on a realistic model of the Solar system obtained from the JPL

ephemeris. In this way, we avoid doing massive numerical simulations on the JPL model that could result in a prohibitive need of computer time.

The motion for a particle in this region is shown in Figure 9. To give a sense of velocity we have drawn the orbit as a polygonal line, putting a vertex for each (Julian) day of integration. From the $(z, \dot{z})$ projections shown in Figure 9, it is clearly seen that the motion in the vertical direction is very close to an harmonic oscillator (with a period of a little less than a month), and that these trajectories reach an approximate angular separation over (or under) the Earth-Moon plane of either 30 or 40 degrees. Note that the trajectories must spend most of the time away from the Earth-Moon plane and near their maximum elongation.

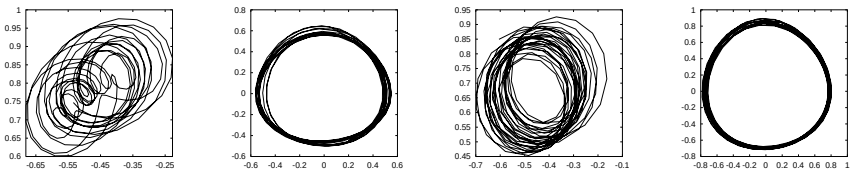

Figure 9. Orbits inside the stable region near L_5, for the JPL model. First plot: (x, y) projection of an orbit with $\dot{z} = 0.58$. Second plot: $(z, \dot{z})$ projection of the previous orbit. Third plot: (x, y) projection of an orbit with $\dot{z} = 0.83$. Fourth plot: $(z, \dot{z})$ projection of the previous orbit. Integration time: 1 year.

References

1. G. Benettin, F. Fassò, and M. Guzzo. *Regul. Chaotic Dyn.* **3(3)**, 56 (1998).
2. Broer, H.W., Hanßmann, H., Jorba, À., Villanueva, J. and Wagener F., *Nonlinearity* **16**, 1751 (2003).
3. A. Celletti and A. Giorgilli. *Celestial Mech.* **50(1)**, 31 (1991).
4. E. Castellà and À. Jorba. *Celestial Mech.* **76(1)**, 35 (2000).
5. J. Cronin, P.B. Richards, and L.H. Russell. *Icarus* **3**, 423 (1964).
6. C. Díez, À. Jorba, and C. Simó. *Celestial Mech.* **50(1)**, 13 (1991).
7. A. Giorgilli, A. Delshams, E. Fontich, L. Galgani, and C. Simó. *J. Differential Equations* **77**, 167 (1989).
8. À. Jorba. *Astron. Astrophys.* **364(1)**, 327 (2000).
9. À. Jorba. *Nonlinearity* **14(5)**, 943 (2001).
10. À. Jorba and J. Villanueva. *Nonlinearity* **10**, 783 (1997).
11. À. Jorba and J. Villanueva. *J. Nonlinear Sci.* **7**, 427 (1997).
12. C. Simó, G. Gómez, À. Jorba, and J. Masdemont. In A.E. Roy and B.A. Steves, editors, *From Newton to Chaos*, pages 343–370, Plenum Press (1995).
13. C. Simó. *Mem. Real Acad. Cienc. Artes Barcelona*, 48(7):303–348, 1989.
14. V. Szebehely. *Theory of Orbits*. Academic Press, 1967.